Magnetic−Noble Metal Nanocomposites with Morphology-Dependent Optical Response

Nicolás Pazos-Pérez,[†] Yan Gao,[†] Michael Hilgendorff,[†] Stephan Irsen,[‡] Jorge Pérez-Juste,[§] Marina Spasova,[||] Michael Farle,[||] Luis M. Liz-Marzán,[§] and Michael Giersig*,[†]

Department of Nanoparticle Technology and Electron Microscopy Group, Center of Advanced European Studies and Research (CAESAR), 53175 Bonn, Germany, Departamento de Química Física and Unidad Asociada CSIC, Universidade de Vigo, 36310 Vigo, Spain, and Fachbereich Physik and Centre for Nano Integration (CeNIDE), Universität Duisburg-Essen, 47048 Duisburg, Germany

Received January 26, 2007. Revised Manuscript Received June 6, 2007

This paper describes the synthesis of noble metal−magnetic nanoparticle composites with different shapes, using a seeded-growth approach in the presence of a cationic surfactant (cetyltrimethylammonium bromide, CTAB). Hydrophobic $CoPt_3$ and FePt nanoparticles were transferred into water using CTAB as a phase-transfer agent and were subsequently used as seeding materials for the reduction of gold and silver precursors to produce Au−$CoPt_3$, Ag−$CoPt_3$, and Au−FePt nanocomposites. The nanocomposites synthesized were characterized by transmission electron microscopy (TEM), UV−visible spectroscopy, and SQUID magnetometry. Through the modification of the growth conditions, Au−$CoPt_3$ nanocomposites with various morphologies (spheres, cubes, rods) were prepared, providing an opportunity to tailor the optical response of these composite nanoparticles while maintaining the magnetic properties of the original seeds, even upon phase transfer into water.

Introduction

The study of nanoscale particles is generally motivated by the change in physical and chemical properties as compared to bulk materials. Depending on the nature of the materials of interest, this change will be mainly manifested in a particular property, which can, for example, be the magnetic response for transition metals such as iron or cobalt, luminescence for semiconductors, or surface plasmon resonance for noble metals. After some 25 years of characterizing many different materials with a variety of sizes and shapes, currently, a major challenge is the implementation of more than one such property at the single particle level, which will allow us to explore new technological applications. Among the many methods for the preparation of nanomaterials, such as chemical vapor deposition or molecular beam epitaxy, the colloid chemistry approach offers a number of advantages, because it allows a tight control of particle size and shape, as well as an easy and reasonably low-cost upscaling. In particular, the wet chemical synthesis of anisotropic nanoparticles (rods and wires) has become of great interest because the materials (optical, electronic, catalytic) properties can be tuned via the control of the shape.[1]

The possibility of creating smart nanosystems containing different sections, each characterized by a different physical property, size, or morphology, has been developed as a consequence of bottom-up nanotechnology methods. These so-called hybrid nanocrystals can be classified into two types: core−shell structures and heterodimers. Core−shell structures comprise a nanocrystalline core covered by a shell of another material and many different types have been obtained through different synthetic protocols. The most widely studied core−shell composites are based on two or more types of semiconductor materials,[2−6] such as CdS@ZnSe or CdSe@ZnS,[4,5] where the shell is grown to enhance the photoluminescence and stability of the core. Other types of composites are based on two or more metals, for instance, Au@Ag,[7] Ag@Co,[8] or bimagnetic core−shell nanocrystals,[9] as well as their combination with insulators, e.g., SiO_2, to produce core−shell composites.[10−12] In each case, the photoluminescence properties, optical properties, and magnetic properties can be improved or modified as compared to those of pure, single-component particles.

* Corresponding author. E-mail: giersig@caesar.de.
[†] Department of Nanoparticle Technology, Center of Advanced European Studies and Research.
[‡] Electron Microscopy Group, Center of Advanced European Studies and Research.
[§] Universidade de Vigo.
[||] Universität Duisburg-Essen.

(1) Liz-Marzan, L. M. *J. Mater. Chem.* **2006**, *16* (40), 3891.
(2) Mews, A.; Eychmuller, A.; Giersig, M.; Schooss, D.; Weller, H. *J. Phys. Chem.* **1994**, *98* (3), 934.
(3) Eychmuller, A.; Mews, A.; Weller, H. *Chem. Phys. Lett.* **1993**, *208* (1−2), 59.
(4) Hines, M. A.; Guyot-Sionnest, P. *J. Phys. Chem.* **1996**, *100* (2), 468.
(5) Dabbousi, B. O.; RodriguezViejo, J.; Mikulec, F. V.; Heine, J. R.; Mattoussi, H.; Ober, R.; Jensen, K. F.; Bawendi, M. G. *J. Phys. Chem. B* **1997**, *101* (46), 9463.
(6) Peng, X. G.; Schlamp, M. C.; Kadavanich, A. V.; Alivisatos, A. P. *J. Am. Chem. Soc.* **1997**, *119* (30), 7019.
(7) Rodriguez-Gonzalez, B.; Burrows, A.; Watanabe, M.; Kiely, C. J.; Liz-Marzan, L. M. *J. Mater. Chem.* **2005**, *15* (17), 1755.
(8) Sobal, N. S.; Hilgendorff, M.; Mohwald, H.; Giersig, M.; Spasova, M.; Radetic, T.; Farle, M. *Nano Lett.* **2002**, *2* (6), 621.
(9) Zeng, H.; Li, J.; Wang, Z. L.; Liu, J. P.; Sun, S. H. *Nano Lett.* **2004**, *4* (1), 187.
(10) Salgueirino-Maceira, V.; Correa-Duarte, M. A.; Farle, M. *Small* **2005**, *1* (11), 1073.
(11) Salgueirino-Maceira, V.; Spasova, M.; Farle, M. *Adv. Funct. Mater.* **2005**, *15* (6), 1036.
(12) Salgueirino-Maceira, V.; Correa-Duarte, M. A.; Spasova, M.; Liz-Marzan, L. M.; Farle, M. *Adv. Funct. Mater.* **2006**, *16* (4), 509.

10.1021/cm070248o CCC: $37.00
Published on Web 08/08/2007

Other types of hybrid structures are heterodimers,[13−16] in which two or more domains are linked through a small interfacial area. Nanocrystal heterodimers can be prepared from materials having a large interfacial energy or when only certain regions on the surface of a starting nanocrystal can be accessed by the second material. As for the core−shell composites, different synthetic protocols have been proposed to obtain heterodimers, such as semiconductor−metallic,[17−19] semiconductor−magnetic,[14] magnetic−metallic,[15,20,21] and metallic−metallic.[15] An important issue in the growth of these kinds of heterodimers is the independent control of the sizes of both domains, making them highly versatile for a number of applications. On a higher complexity level, Shi et al. have proposed a general approach to obtain ternary hybrid nanocrystals.[22] Although significant progress has been made on the preparation of both types of hybrid materials (core−shell and heterodimers), almost all synthetic protocols proposed to date were developed in organic media and under anaerobic conditions.

The work presented here is concerned with the synthesis of composite nanoparticles comprising a magnetic component linked to a noble metal nanoparticle in an aqueous environment, whose size and shape determines the optical response. The production of such nanocomposites was carried out using a modified seeded-growth method, where the seeds were made of magnetic nanoparticles ($CoPt_3$, FePt), previously produced in high-boiling-point organic solvents. The process thus requires transfer into water using the same surfactant (cetyltrimethylammonium bromide, CTAB) that is usually employed to induce anisotropic growth of noble metals. The growth step on the magnetic seeds requires reduction of a gold or silver salt with a weak reducing agent (ascorbic acid) in the presence of CTAB, yielding stable composites of magnetic seeds attached onto gold and silver particles with various morphologies (spheres, cubes, and rods), so that a wide variety of optical properties can be obtained through changes in the nanocomposite surface plasmon resonance frequency for the different shapes. Although the formation of $CoPt_3$−Au dimer nanocrystals was reported earlier,[21] the present method is more versatile because of the use of aqueous surfactant solutions, which allow straightforward variations in the size and shape of the metallic components, which has been developed in a much lesser extent for reactions in organic solvents.

Experimental Section

Chemicals and Apparatus. Diphenyl ether (99%), 1,2-hexadecanediol (90%), 1-adamantanecarboxylic acid (99%, ACA), 1,2-dichlorobenzene (99%), platinum(II)-acetylacetonate (97%, $Pt(acac)_2$), dioctyl ether (99%), oleic acid (90%), oleylamine (70%), iron pentacarbonyl (99.9%, $Fe(CO)_5$), silver nitrate (99.9%, $AgNO_3$) and cetyltrimethylammonium bromide (99%, CTAB) were purchased from Aldrich. Hexadecylamine (92%, HDA) was purchased from Merck; 2-propanol (99.7%), ethanol (99%), chloroform (99%), ascorbic acid (99.5%), and sodium hydroxide (99%, NaOH) were purchased from Roth; dicobalt octacarbonyl ($Co_2(CO)_8$, stabilized with 1−5% hexane) from Strem Chemicals; and tetrachloroauric acid ($HAuCl_4 \cdot 3H_2O$) from Fluka. All reactants were used without further purification. Mili-Q water (18 MΩ cm^{-1}) was used in all aqueous solutions, and all the glassware was cleaned with aqua regia before the experiments.

UV−vis−near-IR spectroscopy (Varian, Cary 500), transmission electron microscopy, TEM (Leo 922A EFTEM, operating at 200 kV), high-resolution TEM (HRTEM) (Philips CM 12, operating at 120 kV), and STEM (ZEISS Libra 200-CRISP, operating at 200 kV) combined with an EDX detector, were applied to characterize the optical response, composition, structure, and size distribution of the synthesized nanocomposites. Magnetic measurements were carried out using a superconducting quantum interference device (SQUID), varying the temperature between 5 and 300 K, according to the typical procedure for the "zero-field-cooling/field-cooling" (ZFC/FC) method in the presence of a relatively weak applied magnetic field (100 Oe). The hysteresis loops at 5 K were obtained by alternating the magnetic field from −20 to +20 kOe. The samples were prepared for the measurements under an inert atmosphere in gelatine capsules.

Synthesis of Magnetic Seeds. $CoPt_3$ and FePt alloy nanocrystals were used as seeds and prepared using the methods previously reported by Shevchenko et al.[23] and by Sun et al.,[24] respectively. The details are summarized as follows:

- $CoPt_3$ nanocrystals were synthesized in a high-boiling-point coordinating solvent under an argon atmosphere. Briefly, 1,2-hexadecandiol (0.13 g, 0.5 mmol), $Pt(acac)_2$ (0.033 g, 0.083 mmol), and ACA (0.25 g, 1.4 mmol) were dissolved in a mixture of HDA (4 g) and diphenyl ether (2 mL). The reaction temperature was increased to 145 °C, and a freshly prepared solution of $Co_2(CO)_8$ (0.043 g, 0.125 mmol) in 1,2-dichlorobenzene (0.6 mL) was injected into the hot reaction mixture. The reaction was maintained at this temperature (145 °C) for 1 h, and thereafter the temperature was increased up to reflux (∼275−285 °C) during 1 h to induce the annealing of the particles. By changing the amount of precursors, surfactants, and injection temperature, we could adjust particle sizes. After being cooled to room temperature, the $CoPt_3$ nanoparticle solution was mixed with chloroform (∼5 mL) and 2-propanol (∼20 mL) and subsequently centrifuged (12 000 rpm, 20 min) so that the precipitate could be easily redispersed in diverse nonpolar solvents such as toluene, hexane, or chloroform. Representative TEM images of the obtained particles and the corresponding size distributions are shown in Figure 1A, C, and E. The mean diameter determined from the mentioned images was 7.97 ± 0.61 nm.

- FePt nanocrystals were synthesized as described in ref 24, using a combination of oleic acid and oleyamine to stabilize the monodisperse FePt colloids and prevent oxidation. The synthesis

(13) Lu, Y.; Xiong, H.; Jiang, X. C.; Xia, Y. N.; Prentiss, M.; Whitesides, G. M. *J. Am. Chem. Soc.* **2003**, *125* (42), 12724.
(14) Gu, H. W.; Zheng, R. K.; Zhang, X. X.; Xu, B. *J. Am. Chem. Soc.* **2004**, *126* (18), 5664.
(15) Gu, H. W.; Yang, Z. M.; Gao, J. H.; Chang, C. K.; Xu, B. *J. Am. Chem. Soc.* **2005**, *127* (1), 34.
(16) Green, M. *Small* **2005**, *1* (7), 684.
(17) Mokari, T.; Rothenberg, E.; Popov, I.; Costi, R.; Banin, U. *Science* **2004**, *304* (5678), 1787.
(18) Cozzoli, P. D.; Manna, L. *Nat. Mater.* **2005**, *4* (11), 801.
(19) Carbone, L.; Kudera, S.; Giannini, C.; Ciccarella, G.; Cingolani, R.; Cozzoli, P. D.; Manna, L. *J. Mater. Chem.* **2006**, *16* (40), 3952.
(20) Yu, H.; Chen, M.; Rice, P. M.; Wang, S. X.; White, R. L.; Sun, S. H. *Nano Lett.* **2005**, *5* (2), 379.
(21) Pellegrino, T.; Fiore, A.; Carlino, E.; Giannini, C.; Cozzoli, P. D.; Ciccarella, G.; Respaud, M.; Palmirotta, L.; Cingolani, R.; Manna, L. *J. Am. Chem. Soc.* **2006**, *128* (20), 6690.
(22) Shi, W. L.; Zeng, H.; Sahoo, Y.; Ohulchanskyy, T. Y.; Ding, Y.; Wang, Z. L.; Swihart, M.; Prasad, P. N. *Nano Lett.* **2006**, *6* (4), 875.
(23) Shevchenko, E. V.; Talapin, D. V.; Schnablegger, H.; Kornowski, A.; Festin, O.; Svedlindh, P.; Haase, M.; Weller, H. *J. Am. Chem. Soc.* **2003**, *125* (30), 9090.
(24) Sun, S. H.; Murray, C. B.; Weller, D.; Folks, L.; Moser, A. *Science* **2000**, *287* (5460), 1989.

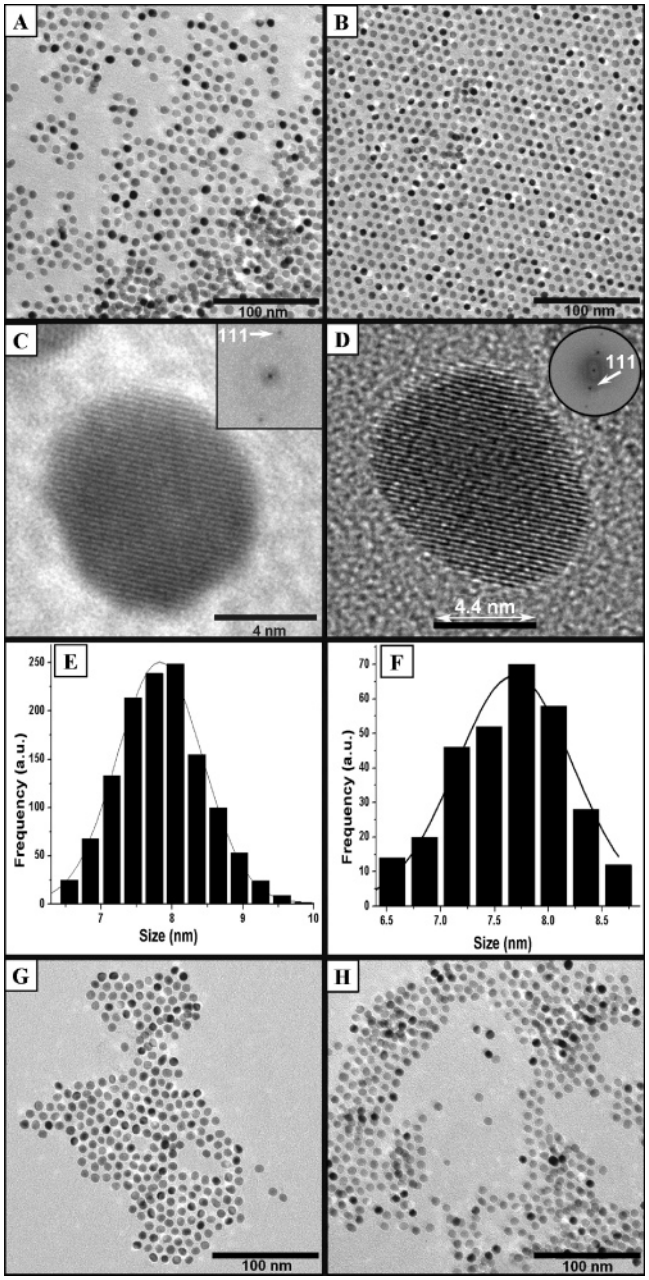

Figure 1. TEM and HRTEM images and particle size distribution histograms of ~8 nm $CoPt_3$ (A, C, and E, respectively) and FePt (B, D, and F, respectively) alloys. TEM images of $CoPt_3$ (G) and FePt (H) alloys after solvent transfer into water.

is based on the reduction of $Pt(acac)_2$ to Pt metal by a diol (1,2-hexadecandiol) and the thermal decomposition of $Fe(CO)_5$ in high temperature solutions to produce Fe^0. The composition of these FePt nanoparticles can be adjusted by controlling the molar ratio between iron carbonyl and platinum salt, whereas particle sizes can be tuned from 3 to 10 nm by first growing 3 nm seed particles and then adding more reagents to enlarge the existing seeds to the desired size. In a typical synthesis, under airless conditions, $Pt(acac)_2$ (0.197 g, 0.5 mmol) and 1,2-hexadecandiol (0.390 g, 1.5 mmol) were dissolved in dioctyl ether (20 mL); oleic acid (0.16 mL, 0.5 mmol), oleylamine (0.17 mL, 0.5 mmol), and $Fe(CO)_5$ (0.13 mL, 1 mmol) were subsequently added to the mixture and heated to reflux (290 °C) for 1 h. The obtained particles, with an approximated size of 4 nm, were used as seeds for a further FePt nanoparticles overgrowth up to the desired size by the addition of more reagents. Upon the mixture being cooled to room temperature, an addition of ethanol (40 mL) leads to precipitation of a black product, which can be separated by centrifugation (12 000 rpm, 20 min) and then redispersed in nonpolar solvents (toluene, hexane, or chloroform were used). Representative TEM images of the obtained particles, as well as their size histogram, are shown in Figure 1B, D, and F, from which a mean diameter around 8 nm was again determined.

Transfer of $CoPt_3$ and FePt Nanocrystals into Water. The transfer of both $CoPt_3$ and FePt nanoparticles from an organic into an aqueous medium was accomplished using CTAB as a phase transfer agent, using a modification of the method developed by Fan.[25]

In a typical procedure, a 5 mL aliquot of the prepared magnetic nanoparticles ($CoPt_3$ or FePt; previously washed as mentioned above and redispersed in 30 mL of a nonpolar solvent) was again centrifuged (7500 rpm, 20 min) upon addition of a bad solvent such as ethanol (80%vol). After redispersion in an organic solvent (with a lower boiling point and a higher density than water) such as chloroform (15 mL), an aqueous CTAB solution (30 mL, 0.1 M) was added, forming a two-phase system with the organic phase below and the aqueous phase on top; the magnetic particles are in the organic phase. This mixture was transferred into a typical distillation setup, followed by evaporation of the organic solvent under vigorous magnetic stirring. After several hours at 90 °C, the chloroform was completely removed from the mixture and a clear nanoparticle aqueous solution was obtained. A final centrifugation step (4000 rpm, 10 min) was performed to remove possible aggregates.

Growth of Noble Metals. We used gold and silver to produce nanocomposites by means of a seeded growth method[26−30] in which the $CoPt_3$ and FePt nanoparticles were used as seeds upon transfer into water.

For gold, the general procedure was as follows: 10 mL of a growth solution containing CTAB (0.1 M) and $HAuCl_4$ (5.00×10^{-4} M) was thermosttated at 25−30 °C, and ascorbic acid (0.075 mL, 0.1 M) was added (observing a color change from orange for Au^{3+}−CTAB complexes into colorless for Au^{+}−CTAB). Next, different amounts of $AgNO_3$ (to decrease the reaction kinetics favoring rod shape formation) were mixed with the growth solution, and finally, selected volumes of seed solution were added. After 1 h, the color of the solution had changed to violet or red depending on the amounts of reagents, reflecting reduction of Au^{+} into Au^0 and formation of the nanocomposites. By independently varying the amounts of $AgNO_3$ and seed, we obtained different shapes and sizes.

For silver, a similar seeded growth method was used, replacing $HAuCl_4$ with $AgNO_3$ and changing the pH of the solution, which is crucial for the reduction of Ag^{+} by ascorbic acid.[27−31] The reaction was hence started by increasing the pH of the solution through NaOH addition (0.2 mL, 0.1 M), followed by quick mixing. After 1 h, it was observed that the color of the solution becomes yellow because of the formation of Ag^0.

For TEM preparation, the excess surfactant present in the particle solution was removed by centrifuging 1 mL of the particle solution at 9000 rpm for 10 min. The supernatant containing surfactant was

(25) Fan, H. Y.; Yang, K.; Boye, D. M.; Sigmon, T.; Malloy, K. J.; Xu, H. F.; Lopez, G. P.; Brinker, C. J. *Science* **2004**, *304* (5670), 567.
(26) Jana, N. R.; Gearheart, L.; Murphy, C. J. *Chem. Commun.* **2001**, (7), 617.
(27) Nikoobakht, B.; El-Sayed, M. A. *Chem. Mater.* **2003**, *15* (10), 1957.
(28) Perez-Juste, J.; Pastoriza-Santos, I.; Liz-Marzan, L. M.; Mulvaney, P. *Coord. Chem. Rev.* **2005**, *249* (17−18), 1870.
(29) Liz-Marzan, L. M. *Mater. Today* **2004**, *7* (2), 26.
(30) Perez-Juste, J.; Correa-Duarte, M. A.; Liz-Marzan, L. M. *Appl. Surf. Sci.* **2004**, *226* (1−3), 137.
(31) Perez-Juste, J.; Liz-Marzan, L. M.; Carnie, S.; Chan, D. Y. C.; Mulvaney, P. *Adv. Funct. Mater.* **2004**, *14* (6), 571.

Table 1. Details on Amounts of Different Reactants Used To Produce Nanocomposites with Various Shapes and Sizes

	small spheres	large spheres	cubes	small rods	medium rods	large rods
CTAB (M)	0.10	0.10	0.27	0.10	0.10	0.10
$HAuCl_4$ (mM)	0.25	0.50	0.50	0.25	0.50	0.25
Asc. Ac. (mM)	0.37	0.75	0.75	0.37	0.75	0.37
$AgNO_3$ (mM)			0.02	0.02	0.05	
$CoPt_3$ seeds (μL)	1000	200	200	2500	200	25

discarded and the precipitate was redispersed in 1 mL of water. It was again centrifuged and redispersed in 1 mL of water. Next, a drop of the particle solution was placed on a carbon-coated copper grid and dried at room temperature.

Detailed conditions for the preparation of diverse morphologies (spheres, cubes, and rods) and sizes from $CoPt_3$ seeds are summarized in Table 1.

Results and Discussion

Characterization of Magnetic Seeds. The transmission electron microscopy (TEM and HRTEM) observation of the $CoPt_3$ nanocrystals has confirmed high monodispersity and crystallinity (images A and C in Figure 1) with well-separated nanocrystals on the TEM images and lattice fringes without stacking faults observable in HRTEM. The particle size distribution shown in Figure 1E was obtained from statistical evaluation of nanocrystals from several TEM images (~1200 particles), and these measurements confirm a relatively narrow and nearly symmetric distribution with an average particle size of 7.97 nm and a standard deviation of 0.61 nm.

A similar TEM and HRTEM characterization was carried out on FePt nanocrystals, which again confirm high monodispersity and crystallinity (images B and D in Figure 1). The particles are single crystals with the characteristic (111) lattice planes for the chemically disordered face-centered cubic (fcc) FePt phase, and the average particle size determined by statistical analysis of TEM images (~300 particles) was 7.74 nm with a standard deviation of 0.52 nm (Figure 1F).

Because the growth of noble metals was to be carried out in aqueous CTAB solutions, prior transfer of the magnetic nanoparticles into water was required. This was successfully achieved by a modification of a reported two-phase system evaporation method,[25] as described in the experimental section. To confirm that phase transfer occurred without significantly affecting the colloidal stability, we characterized the $CoPt_3$ and FePt from aqueous dispersions again by TEM and HRTEM, revealing identical morphology and structure before and after the transfer, with no aggregation, as shown in images G and H of Figure 1.

$CoPt_3$−Au Nanocomposites. For the preparation of $CoPt_3$−Au bifunctional nanocrystals, the popular seeded growth method[26−30] was used, with CTAB not only acting as a stabilizer for the colloids but also facilitating transport of Au ions and directing anisotropic growth.[31] The main difference with the standard seed-mediated growth was the use of the magnetic alloys ($CoPt_3$) as seeds. As detailed in the Experimental Section, changes in different reaction parameters, such as CTAB, gold salt, and silver nitrate concentrations, lead to growth of Au particles with different shapes (spheres, cubes, and rods) from the $CoPt_3$ seeds, (see Table 1).

Spherical Au Particles. Spherical Au particles were obtained in the absence of silver nitrate while the surfactant concentration was kept constant and the $[Au^{3+}]$:[ascorbic acid] ratio was equal to 1:1.5. The average sphere size could be tuned through variation of the relative amounts of gold salt and seed particles, because a larger amount of seed particles means more nucleation points available and thus smaller final spheres (Figure 2A). On the contrary, by increasing the Au^{3+} concentration, the final sphere diameter is clearly increased, as can be seen in Figure 2B. The precise morphology of these spherical $CoPt_3$−Au nanocomposites was determined by tilting the sample within the TEM, from 0 to 30° in 10° steps, with respect to the electron beam (see Figure 2C−F). The results clearly reveal that the growth of gold takes place exclusively on one side of the magnetic seeds, with the final result of one $CoPt_3$ alloy nanoparticle located on the surface of the (larger) gold sphere. Figure 3 shows the absorbance spectra of two $CoPt_3$−Au spherical

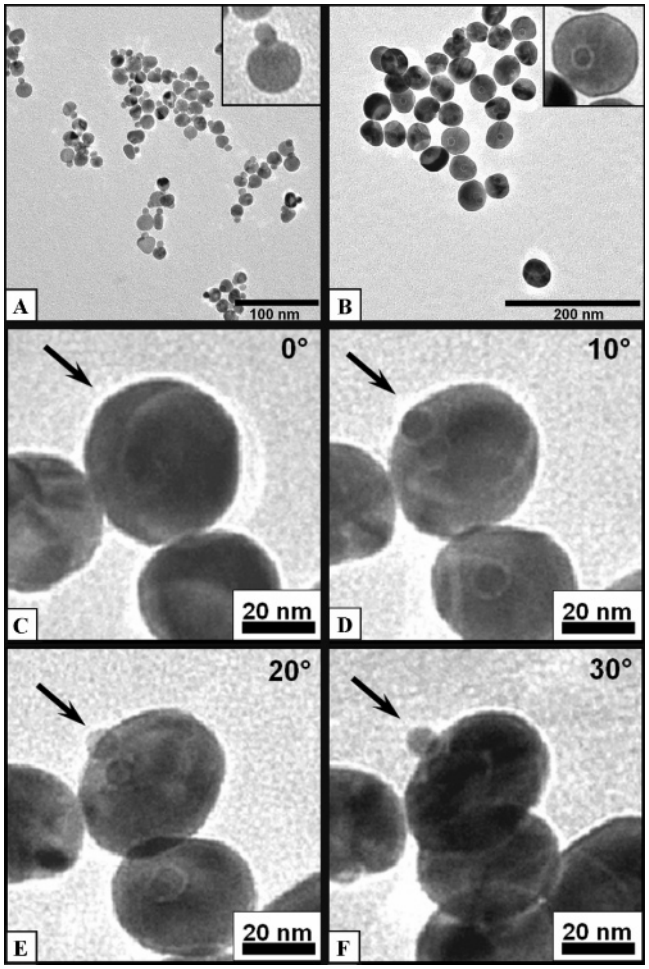

Figure 2. TEM images of spherical $CoPt_3$−Au nanocomposites: small (~15 nm, A) and large (~40 nm, B) and TEM images of spherical $CoPt_3$−Au nanocomposites in a tilting sequence of the sample from 0 to 30° (C−F), with respect to the electron beam.

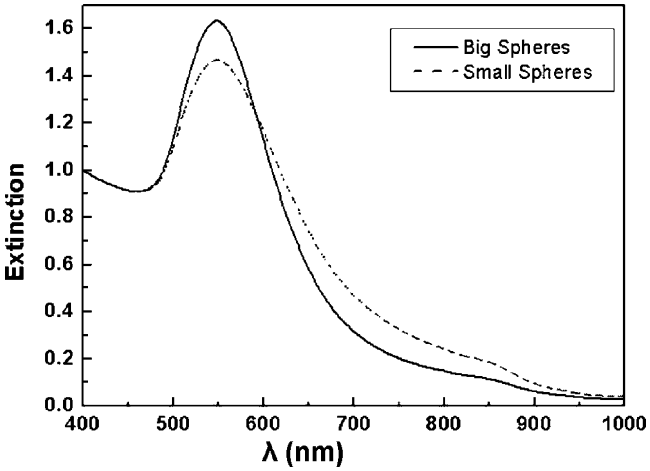

Figure 3. Extinction spectra for aqueous dispersions of spherical $CoPt_3$−Au nanocomposites with two different diameters; 15 and 40 nm. The spectra were normalized to equal absorbance at 400 nm for clarity.

nanocomposites, representative of different particle sizes, as shown in TEM images A and B in Figure 2. The position of the maximum (around 550 nm) is basically co-incident for both samples, but larger particles have a larger extinction cross section, as expected from theory.[32] The slightly red-shifted plasmon resonance most likely arises as a result of small deviations from the spherical geometry, as can be observed in the TEM images. To confirm the nature of the synthesized nanocomposites, we performed a more detailed electron microscopy characterization by means of STEM-EDX analysis to determine the elemental composition of the produced heterodimers. To this end, nanocomposites with small Au spheres (∼8 nm) were used to equalize the intensities of the materials in the EDX analysis. Figure 4 shows the EDX mapping analysis and a TEM image of the same particle in which the gold distribution (red) can be clearly seen. The green and blue colors belong to Pt and Co, respectively. The corresponding energy spectrum is also shown in this Figure.

Cubic and Rodlike Shaped Composites. Cubic and rod-shaped composites were produced in the presence of silver nitrate, which has been shown to reduce the reaction kinetics and induce rod formation.[27−34] It has been found that although a 0.1 M CTAB concentration invariably yielded formation of rods (Figure 5A−C), with an increase in surfactant concentration (∼0.3 M), cubic structures were obtained (Figure 5D). The size and aspect ratio of the rods can be varied through the amount of seed particles and gold salt added, in a similar fashion to what was observed for spheres (see above). Figure 6 shows the absorbance spectra for cubic and rod-shaped nanocomposites. Although just one resonance band dominates the spectrum for cubes,[35] both rod samples show two bands arising from transverse and longitudinal resonances. However, the polydispersity of these samples and the presence of other shapes (mostly spheres) contribute to an unexpected shape for the spectra, with predominance

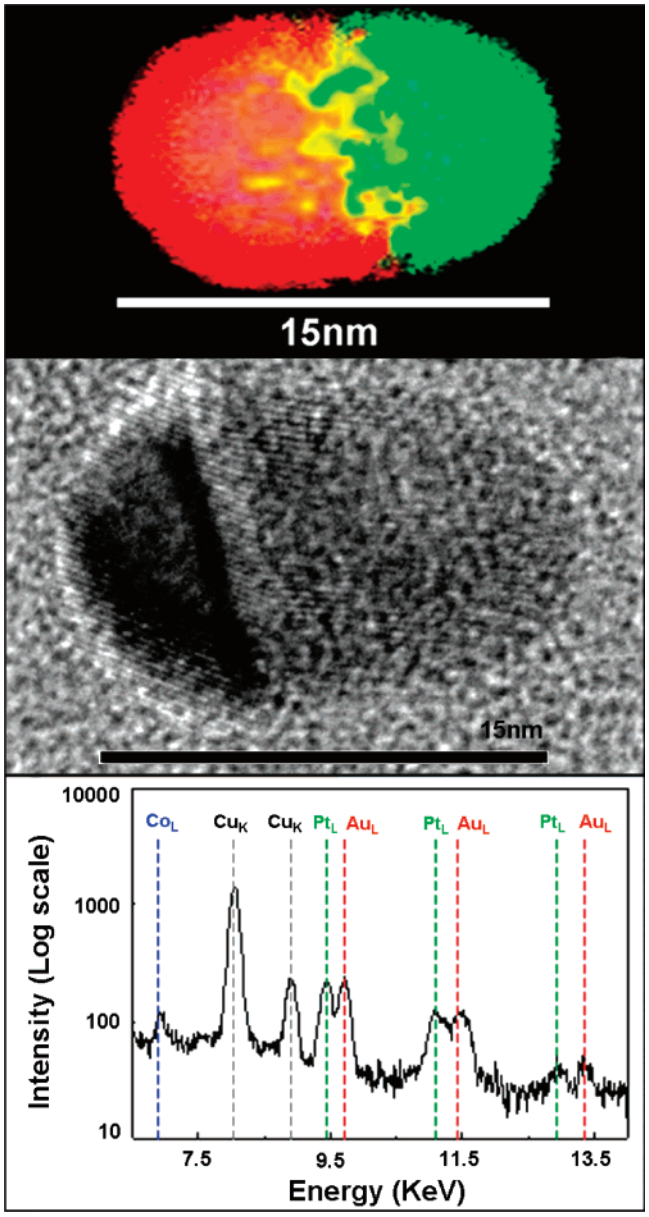

Figure 4. EDX mapping analysis, TEM image (where the typical lattices plane of gold are very well resolved), and the corresponding energy spectrum of $CoPt_3$−Au nanocomposites ($CoPt_3 \approx 8$ nm and Au ≈ 8 nm). Colors in the spectrum correspond to the same elements in the mapping. The Cu in the energy spectra belong to the Cu grid used for TEM investigations.

of the transverse plasmon resonance. In the case of the short rods, the presence of elongated spheres leads to a second band close to that of spheres.

$CoPt_3$−Ag Nanocomposites. The synthesis of $CoPt_3$−Ag nanocomposites was performed using the same strategy as for gold composites. As shown in Figure 7A, pseudo-spherical silver particles were grown, for which a single plasmon band was to be expected. This is confirmed in Figure 7C, where the absorbance spectrum for $CoPt_3$−Ag nanocomposites is observed, displaying a nearly symmetric absorption band around 410 nm. This system has not been studied in detail, and the results presented here are intended only to show the possibility of growing silver on the $CoPt_3$ alloys in a similar fashion to gold.

(32) Bohren, C. F.; Huffman, D. R. *Adsorption and Scattering of Light by Small Particles*; Wiley-Interscience: New York, 1983.
(33) Liu, M. Z.; Guyot-Sionnest, P. *J. Phys. Chem. B* **2004**, *108* (19), 5882.
(34) Liu, M. Z.; Guyot-Sionnest, P. *J. Phys. Chem. B* **2005**, *109* (47), 22192.
(35) Fuchs, R. *Phys. Rev. B* **1975**, *11* (4), 1732.
(36) Antoniak, C.; Lindner, J.; Salgueirino-Maceira, V.; Farle, M. *Phys. Status Solidi A* **2006**, *203* (11), 2968.

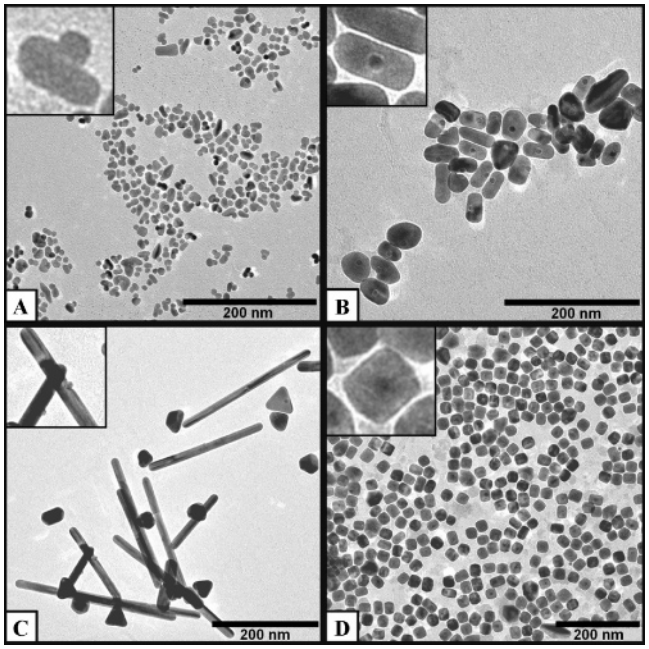

Figure 5. TEM images of $CoPt_3$−Au nanocomposites with two different morphologies, rods (A−C) and cubes (D). See text for details. (A−C) rods with different sizes of (A) 15 × 6 nm, (B), 50 × 20 nm, and (C) 300 × 20 nm. (D) Cubes with a 30 nm side length.

FePt−Au Nanocomposites. Again, the synthesis of FePt−Au was achieved using the same process as described above for $CoPt_3$−Au. We only show here TEM (Figure 7B) and UV−vis (Figure 7C) data to confirm the success in production of nanocomposites using FePt alloys as seeds for gold reduction.

Magnetic Characterization. Magnetic characterization (see details in the Experimental Section) was carried out on both the $CoPt_3$ seeds and the $CoPt_3$−Au nanocomposites, with the aim of investigating the influence of solvent exchange and gold nanoparticle growth on the magnetic properties of $CoPt_3$.

As a representative example of the results, in Figure 8, we show the hysteresis loops measured at 5 K for both $CoPt_3$ nanoparticles and Au−$CoPt_3$ cubic nanocomposites. Both samples show the typical hysteresis loops of an ensemble of superparamagnetic particles in the blocked state. The magnetization curves have been normalized to their respective saturation magnetization M_S at $B = 5$ T. The normalized remanent magnetization ($B = 0$) is the same (0.43 and 0.44) for both $CoPt_3$ and $CoPt_3$−Au. The coercivity exhibited is very similar in both cases, 600 Oe for the $CoPt_3$ seeds and 665 Oe for the cubic $CoPt_3$−Au nanocomposites.

Zero-field-cooled/field-cooled magnetization measurements (Figure 9) show that the blocking temperature for $CoPt_3$ is around 30 K, as reported earlier,[36] and it coincides for the $CoPt_3$−Au nanocomposites. A gradual decay of the magnetization is observed for increasing temperature, which indicates that these particles are superparamagnetic and interact weakly with each other. From these curves (ZFC/FC), one can estimate that both types of particles have a Curie temperature around 300 K.

When examining the obtained results, it can be concluded that the growth of gold on the $CoPt_3$ seeds only marginally affects the hysteresis loop, indicating that their magnetic properties are very similar; it therefore seems that the gold crystal does not affect the magnetic anisotropy of the $CoPt_3$ particles.

Growth Mechanism. The mechanism underlying the formation of these nanocomposites is based on the nucleation of gold on either $CoPt_3$ or FePt nanocrystal surfaces. Ascorbic acid is the reducing agent, and the magnetic platinum alloys serve as nucleation points where the redox reaction takes place. It has been repeatedly shown that ascorbic acid is not strong enough, in the presence of CTAB, to reduce Au^{3+} to Au^0 if no metal seeds are present.[31] However, reduction of Au^{3+} into Au^{1+} can be promoted by ascorbic acid. This is probably related to a high energy barrier for the nucleation of gold in solution when it is complexed with the CTAB monomers, whereas the barrier for gold nucleation on preexisting nuclei is much lower.

We therefore exclude a mechanism in which nucleation of isolated Au nanocrystals is followed by their attachment onto existing magnetic platinum alloy nanocrystals, because control experiments demonstrated that gold does not nucleate in the absence of magnetic platinum alloys. Additionally, a mixture of preformed Au nanoparticles and magnetic platinum alloy nanocrystals, under the same experimental condi-

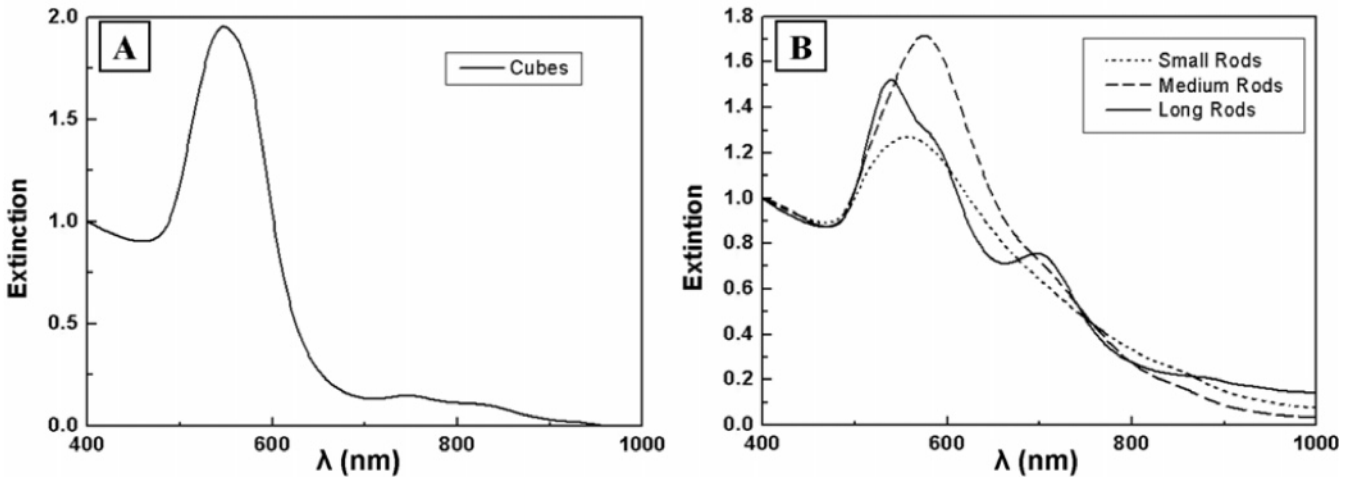

Figure 6. Extinction spectra from cubic (A) and rod-shaped (B) $CoPt_3$−Au nanocomposites. The spectra have been normalized at 400 nm for clarity. See text for details.

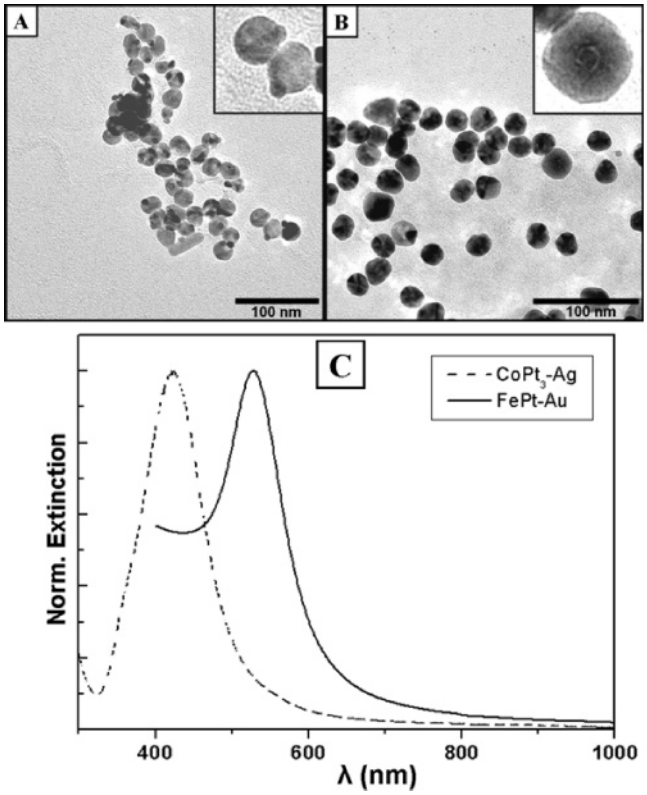

Figure 7. TEM images of (A) $CoPt_3$−Ag and (B) FePt−Au nanocomposites and their corresponding normalized extinction spectra for the aqueous dispersions as indicated in the labels.

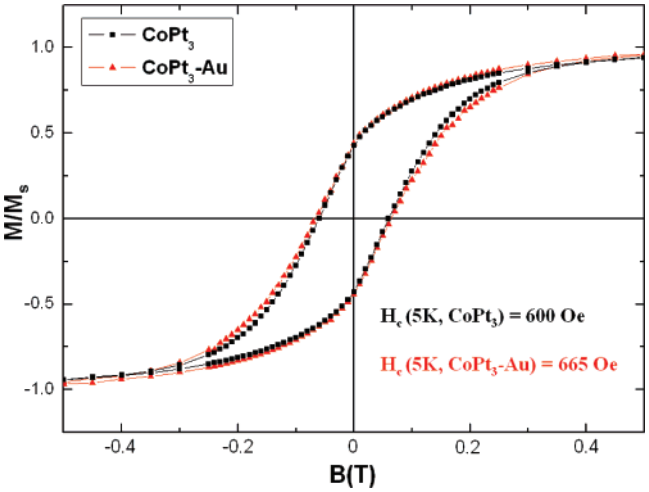

Figure 8. Normalized hysteresis loops obtained for $CoPt_3$ seeds (black) and $CoPt_3$−Au nanocomposites with cubic morphology (red).

tions, does not lead to nanocomposite formation. A final argument against a fusion mechanism is the observation of composites invariably containing two nanoparticles (one made of gold, another of the corresponding alloy), whereas random aggregation should involve more than two particles in a finite number of events.

Regarding morphology control, different sizes and shapes can be obtained through adjustment of certain parameters. Larger nanocomposites require an increase in the concentration of Au or Ag ions, as compared with the amount of seeds (magnetic platinum alloys). The shape can be controlled by controlling the reaction kinetics. When the reaction is faster, it leads to a spherical shape, and when it is slower, cube and rod shapes can be obtained; the slower growth rate may allow the gold atoms to be deposited at the energetically most favorable surface site.[34] The addition of Ag^+ ions or a noticeable increase in the surfactant concentration result on slower kinetics. The increase in the surfactant concentration reduces the reaction rate because of the presence of a larger amount of micelles, which are not all complexed to Au ions, leading to a lower frequency of collisions between complexed micelles and seeds. The addition of silver ions is probably even more efficient in reducing the reaction rate, because of the possibility for Ag^+ to form a compact silver monolayer over the gold surface, preferably on the {110} facets, preventing further growth. This Ag monolayer can be oxidized and replaced by the gold ions from solution; however, the growth rate of gold on {110} facets may be significantly slowed down, whereas {100} facets are only partially covered with silver, and therefore grow faster, which leads to one-dimensional growth along the [100] direction, leading to nanorod formation.[21]

One of the open questions in this work is why the Au crystal does not completely cover the magnetic platinum alloys, forming a core−shell structure, but rather grows only on one particular spot. This could be due to the presumably high interfacial energy between Au and magnetic platinum alloys. The Au starting point of growth would be localized on the facet that minimizes the interfacial energy, and as soon as Au has nucleated on this facet of the magnetic platinum alloys, it is much easier for the additional Au^{1+} ions remaining in the solution to be reduced on the Au^0 already formed rather than on the magnetic platinum alloys because of a self-catalyzed reduction of the gold ions. On a similar system, Pellegrino et al.[21] have observed that the

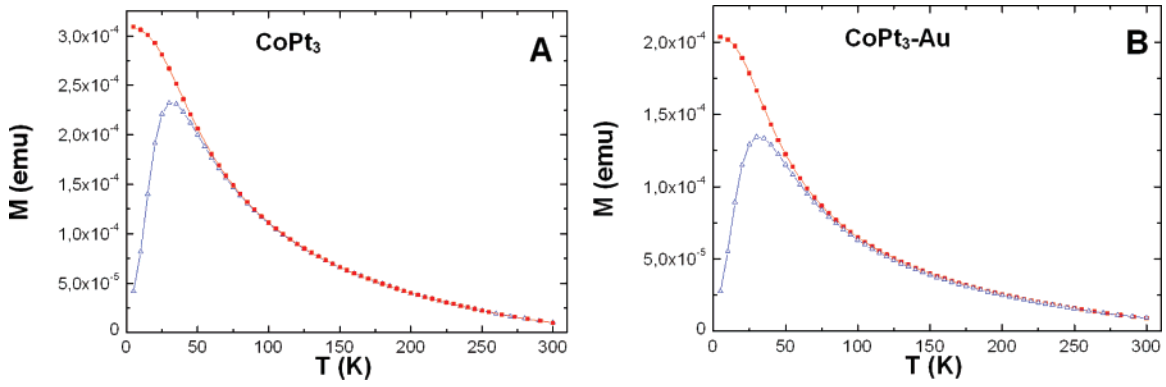

Figure 9. ZFC/FC (blue/red) curves of (A) $CoPt_3$ seeds and (B) for the $CoPt_3$−Au nanocomposites.

growth of Au on small $CoPt_3$ nanoparticles appears to be promoted on the {111} facets, which has the highest growth rate[23] and therefore the highest chemical reactivity, whereas the other facets can be simply less reactive, or not even well-developed. However, an increase in the $CoPt_3$ size decreases the difference in the chemical reactivity among the different facets, and therefore, Au does not show any preference on which facet to grow. They point out that in the seed-catalyzed metal synthesis, the characteristics of the seed, such as its size, surface defects, and the nature of the bound surfactant, dictate the structure of the resulting nanoparticle.

Conclusions

In summary, we have shown that highly monodisperse magnetic platinum alloys (e.g., $CoPt_3$, FePt) synthesized in organic solvents can be transferred into water while still retaining their monodispersity and morphology and can subsequently be used as seeds for growth of noble metals such as Au or Ag. Additionally, the resulting shape of these noble metals can be tuned in different morphologies, forming nanocomposites with diverse structures, including spheres, cubes, or rods, through variation of three different parameters: concentration ratio between noble metal cations and nucleation seeds (magnetic platinum alloys); surfactant concentration; and addition of silver ions, which affect the reaction kinetics. This choice of morphology allows us to obtain magnetically active nanoparticles with a tunable optical response in an aqueous environment, which should find applications in biological and medical research.

Acknowledgment. We thank Izabela Firkowska for useful comments, Thomas Büsgen for helping with the measurements, Ulrike Bloeck (Hahn-Meitner-Institut, Berlin) for HRTEM images, and Antje Thielen and Stephan Maurer (Fachhochschule Bonn-Rhein-Sieg) for analytical measurements. This work was supported by the Marie Curie Research Training Network SyntOrbMag (Contract MRTN-CT-2004-005567).

CM070248O